Australian Journal of Crop Science AJCS

AJCS 17(2):223-232 (2023) ISSN:1835-2707
doi: 10.21475/ajcs.23.17.02.p3802

A new soil-plant image segmentation approach using K-means applied to experimental plots

Danilo Pereira Barbosa[1], Cristiano Ferreira Oliveira[2], Luiz Alexandre Peternelli[2*]

[1]Instituto Federal Goiano, Brazil
[2]Department of Statistics, Universidade Federal de Vicosa, Viçosa, MG, 36570-900, Brazil

***Corresponding author: peternelli@ufv.br**

Abstract

The image segmentation procedure is fundamental in the phenotyping of plant images. Supervised algorithms have been used for pixel soil plant segmentation. Recent research has used the K-means algorithm to evaluate the segmentation of agronomic images in different crops with different databases. The algorithm has shown good performance in the pixel clustering process despite not being able to classify them directly. The present research intends to propose using the K-means algorithm in image segmentation and pixel classification in sugarcane images. 37,430-pixel samples referring to soil and vegetation were manually extracted from some images. This information was used to train and evaluate supervised models. The model with the best performance was considered the "standard" model. A rule that can serve as empirical support to interpret the clusters formed by K-means by assigning a label to each pixel was proposed. Then K-means was used to segment all images and classify the pixels. The vegetation index was used as features and the standard model classification was used as a true label. The measures recall, F1Score, precision, and accuracy were used as a performance measure of K-means, and the mask of each produced to compare the final result of the two approaches, highlighting the vegetation. Using K-means provided better-defined edges than Logistic Regression (standard model) and considerably distinguished the occurrence of soil between the leaves, with precision ranging from 0.77 to 0.92. These results expressed the importance of vegetation index to the clusterization process and showed that K-means ally to an interpretation clusters rule, which could be used to classify pixels in images.

Keywords: Vegetation indices. RGB images. Phenotyping.
Abbreviations: AUC_Area Under de Curve; CIVE_Colour Index of Vegetation Extraction; COM1_Combined Indices 1; COM2_ Combined Indices 2; CNN_ Convolutional Neural Networks; ExG_ Excess of Green; ExGR_ Excess Green minus Excess Red Index; ExR_ Excess Red Index; FN_ False Negative; FP_ False Positive; GLI_ Modified Green Red Vegetation Index; LR_ Logistic regression; MExG_ Modified Excess Green Index; MGVRI_ Modified Green Red Vegetation Index; MPRI_ Modified Photochemical Reflectance Index; NGRDI_ Normalised Green–Red Difference Index; RF_ Random Forest; RGVBI_ Red Green Blue Vegetation Index; ROI_ Region of Interest; TN_ True Negative; TP_ True Positive; VEG_ Vegetativen or vegetative; XGBoost_ Extreme Gradient Boosting.

Introduction

The image segmentation procedure is critical as it enables the extraction of plant phenotypic characteristics from images (Ge et al., 2016; Hamuda et al., 2016; Guo et al., 2021). Image segmentation is a highly relevant task in the field of computer vision. It allows for identifying and classifying areas of interest in the images and quantifying. Numerous pieces of research have shown several applications with its use, enabling the detection of foliar diseases of cucumber, cotton weeds, sweet potato seedlings, and Arabidopsis, among others (Ma et al., 2017; S. Zhang et al., 2019; Guo et al., 2021; Lu et al., 2022).

Bai et al. (2017) used fuzzy clustering segmentation based on grayscale information from images to define cucumber leaf spot diseases. Lu et al. (2022) used color images for robust segmentation of cotton weeds, sweet potato seedlings, and Arabidopsis based on image contrast optimization. The same author used the color indices ExG (Woebbecke et al., 1995), ExR, ExGR (Meyer and Neto, 2008), CIVE (Kataoka et al., 2003), MExG (Burgos-Artizzu et al., 2011), NGRDI (Hunt et al., 2005), VEG (Hague et al., 2006), COM 1 and COM 2 (Guerrero et al., 2012) as a fundamental step in the segmentation process.

Barbosa et al. (2019) used the GLI (Modified Green Red Vegetation Index), MPRI (Modified Photochemical Reflectance Index), RGVBI (Red Green Blue Vegetation Index), ExG (Excess of green), and VEG (Vegetativen) indices to identify soil and exposed vegetation. (emerald grass – Zoysia Japonica). Although all indices were affected by the area's lighting variability, the MPRI and MGVRI showed better discrimination between classes. Concepcion et al. (2022) also evaluated different indices. They attributed greater importance to ExG and RGBVI regarding the efficiency in indicating moisture stress in the canopy of aquaponic lettuce leaves.

It is common to use vegetation indices in image segmentation. These enhance the contrast of plants with other objects in the image, softening lighting effects (Lu et al., 2022). Using these indices allows the broad applicability of different techniques for the segmentation process. Deep learning techniques have been used for this purpose (Lee et al., 2018; Barth et al., 2019; Zheng et al., 2019; Adams et al., 2020; Zhou et al., 2020). However, supervised learning techniques require much image information for the model training process (Henke et al., 2021). Additionally, many images are not always possible since the labels (the class to which each pixel of the training database) must be manually built.

Among the diversity of techniques in this process, the K-means algorithm is famous for presenting characteristics such as agility, efficiency in forming clusters in both small and large data sets, and robustness to outliers (Arai and Barakbah, 2007; Reza et al., 2019). Recent research highlights the use of the K-means algorithm in the evaluation of the segmentation of images obtained from different crops (Zhang et al., 2019; Chouhan et al., 2021; Guo et al., 2021; Henke et al., 2021; Sodjinou et al., 2021; Zhang and Peng, 2022; Lu et al., 2022). However, unlike supervised techniques that assign interest labels to each pixel, the K-means procedure only determines the number of clusters to split on the image. After finishing the clustering process, the researcher is required to interpret them so that it is possible to assign a label to each pixel. This interpretation is often made visually by comparing the actual and cluster images.

In addition, there are no indications of the use of this algorithm in the segmentation of images obtained by drones in experimental fields of genetic improvement. The segmentation of images of crops in this situation allows the evaluation of phenotypic characteristics in the different phases of studies for the selection of potential individuals. The present research intends to propose an approach based on K-means allied to an empirical rule of interpretation of its clusters and then to compare its performance to supervised algorithms with the purpose of segmentation and classification of sugarcane image pixels. The images were obtained using a drone in an experimental research field on sugarcane plant genetic improvement.

Results and discussion

Supervised models evaluation

Initially, we evaluated the supervised models LR, XGBoost, and RF, considering only the R, G, and B channels in the pixels classification for defining the vegetation and soil classes. The models presented outstanding performance (accuracy 0.96) similar to each other. However, in terms of computational effort (Figure 1), the LR model showed the best results.

Subsequently, we repeated the same analysis using only the vegetation indices. A moderately superior performance is noticed only for the XGBoost model (accuracy 0.97), comparing the previous result in which the RGB channels with an accuracy of 0.96 were used. However, despite this slight improvement, the LR model remains the preferred model, since it still presents a significant difference in computational cost from the others (Figure 2).

Considering the model performance, the LR model was chosen as a standard (accuracy 0.96 and shorter execution time) to evaluate the performance of K-means^{+}.

Unsupervised model evaluation

Unlike only the R, G, and B bands, the K-means algorithm presented excellent performance using vegetation indices (Figure 3). These results (Figure 3) express the fundamental role of the indices in highlighting the vegetation present in the experimental plot. It is essential to highlight the tremendous reduction in the number of false positives, 18714 false positives when using only R, G, and B against 126 false positives when using the indices. The number of false negatives also significantly reduced, going from 7102 occurrences to 3711 when using the indices. In all metrics evaluated, there was a significant difference. Correct pixel classification has been increased by 59%. The percentage among all vegetation pixels correctly predicted in the model was increased by more than 100%, and the proportion of pixels classified as vegetation in the actual amount of vegetation pixels increased by 4.6 times. Equivalently, there was a considerable increase in the harmonic mean (F1 Score = 0.92) between precision and recall.

Empirical rule to interpret the clusters

The pixel distribution values for each attribute used were evaluated for the empirical process of determining the class related to each group formed by K-means and then defining the approach that we called K-means^{+}. Among the attributes evaluated, there is a more significant distinction between the soil and vegetation classes when considering the indices (Figure 4). Vegetation indices can highlight a stipulated

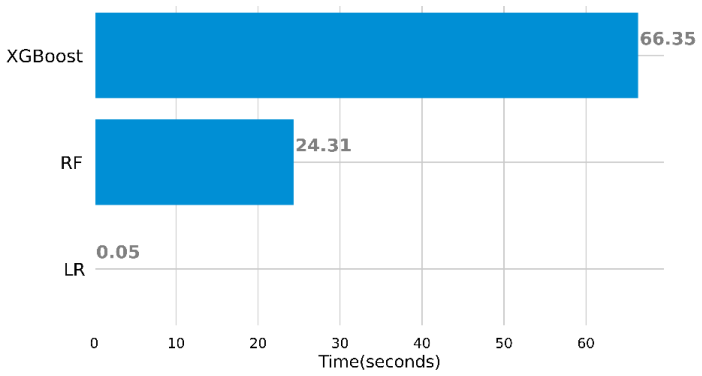

Figure 1. Time spent in the optimization process and model training: logistic regression (LR), XGBoost, and Random Forest (RF) using, as predictor variables, the R, G, and B bands.

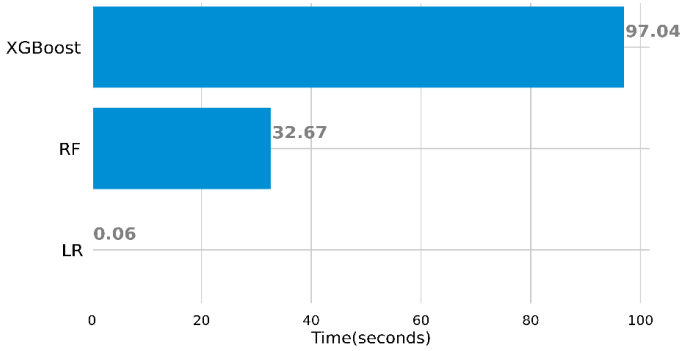

Figure 2. Time spent in the optimization process and model training: logistic regression (LR), XGBoost, and random forest (RF) using vegetation indices as predictor variables.

color (Woebbecke et al., 1995), making it possible to identify the plant in contrast to the soil (Meyer and Neto, 2008). This discrepancy occurs because they attenuate the luminosity and intensify the difference between backgrounds (Campbell and Wynne, 2011).

Note that the attributes that separate the classes easily are those with minor areas of overlap between the soil and vegetation distribution curves. This overlap corresponds to the sum of the false positive and false negative rates. Equivalently, to define a metric for choosing the attribute that allows for the best distinction between classes, the absolute value of the standardized variable z was considered:

$$|z| = abs\left(\left(m_{soil} - m_{vegetation}\right) \Big/ \sqrt{\frac{\sigma 2_{soil}}{n_{soil}} + \frac{\sigma 2_{vegetation}}{n_{vegetation}}}\right)$$

Table 1 presents the values obtained. Higher values of |z| are linked to more easily separable distributions of values. As can be seen, the indices demonstrate better performance than the R, G, and B bands. In addition, among the indices, the one with the highest value is the MGVRI. Therefore, it was used as a criterion to define the class of groups.

The class with the lowest average of MGVRI was assigned the soil label, and the class with the highest average was the vegetation label, as seen in Figure 5. In this way, it was possible to set the black color to mask the pixels belonging to the soil class in the images.

Evaluation of models in image segmentation

Henke et al. (2021) used K-means in plant segmentation and phenotyping using the kmSeg tool. The authors achieved an average of 96% to 99% accuracy when comparing actual data in different image databases. In optimizing the K-means cluster, those authors used additional pre-processing, filtering, and ROI masking steps. However, despite the high values for accuracy, some images were recorded in controlled environments. In contrast, others were recorded in an open environment without a drone.

Taha et al. (2022) used a convolutional neural network (CNN) to study nutritional deficiencies based on imaging plants cultivated in aquaponics. The authors compared CNN with K-means. Despite CNN presenting optimal accuracy and F1Score values greater than 99%, K-means presented values greater than 83% in these evaluated metrics. CNN's prominence regarding K-means was expected, as deep learning algorithms present better results in large data sets (Henke et al., 2021). Similar values to these were also observed with K-means in the dataset of two images of sugarcane, obtained with a drone, from the experimental field in genetic improvement of this study (Figure 5 and Figure 6).

The presented images exemplify the best (Figure 5) and the worst (Figure 6) performance of K-means^{+}. In both scenarios, the efficiency of K-means in segmentation is noticeable. With K-means^{+}, the edges became better defined and the occurrence of soil in

Table 1. Absolute z values calculated for each attribute.

Index	GVRI	PRI	LI	xG	GVBI	EG	ed	reen	lue
$\|Z\|$	81.71	76.95	63.82	47.25	27.26	87.5	9.56	0	0.38

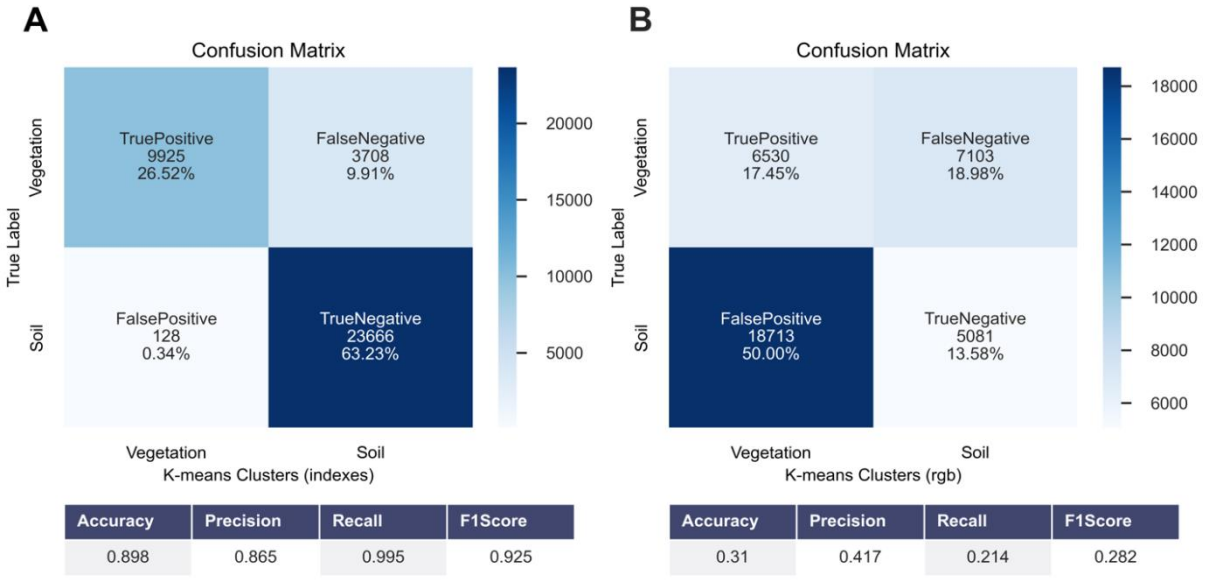

Figure 3. Evaluation metrics and confusion matrix of clusters formed from k-means when using the (A) vegetation indices or (B) only the R, G, and B bands.

the middle of the vegetation was better discriminated in the masking process. These results show the potential of K-means⁺ for image segmentation obtained from plots of field experiments. It also emphasizes the importance of vegetation indices in the pixel clustering process and as an essential tool that can be used to classify the groups formed by K-means.

Materials and methods

Data

The images were collected from an experiment conducted in 2019 at the Sugarcane Research and Improvement Center (CECA) of the Federal University of Viçosa – UFV, located in the municipality of Oratórios – MG, Brazil. The images were obtained from this experiment (Figure 1) with a DJI Phantom 4 UAV-RPA drone. This drone was equipped with an RGB camera (R, red; G, green; and B, blue) with a resolution of 12 megapixels and a focal length of 3.61 mm. The flight was conducted on 03/15/2019 between 11:00 am and 1:00 pm. The six images used in this research (Figure 7) correspond to diverse samples of the original images. These were chosen to have a variability of possible situations when images are collected directly in the field. We have, as extremes, an image with more soil and less developed plants (Figure 7-F) and an image where plants occupy almost the entire plot area (Figure 7-E).

Images processing

From those six images (Figure 7), pixel samples were extracted with their respective classes (soil and vegetation). These samples were used in structuring a two-dimensional table (data frame) for subsequent analyses.

The six images (Figure 7) were used to manually extract pixels corresponding to the soil and vegetation classes. From these images, 37430 pixels were manually extracted. The corresponding values of the red (R), green (G), and blue (B) bands were saved in the columns of a data frame, accompanied by the corresponding class (soil or vegetation). The R, G, and B bands were used to calculate the vegetation indices GLI, MPRI, RGVBI, ExG, and VEG that were saved in new columns of the same data frame. These indices are defined as:

Modified Green Red Vegetation Index: $GLI = \frac{2G-R-B}{2G+R+B}$ (Louhaichi et al., 2008);

Modified Photochemical Reflectance Index: $MPRI = \frac{G-R}{G+R}$ (Yang et al., 2008);

Red Green Blue Vegetation Index: $RGVBI = \frac{G-(B*R)}{G^2+(B*R)}$ (Bendig et al., 2015);

Excess of green: $ExG = 2G - R - B$ (Woebbecke et al., 1995);

Vegetation: $VEG = \frac{G}{R^a * B^{(1-a)}}$, where $a = 0.667$ (Hague et al., 2006).

The columns composed of bands and vegetation indices were named attributes in this data frame. The columns corresponding to the class of pixels were

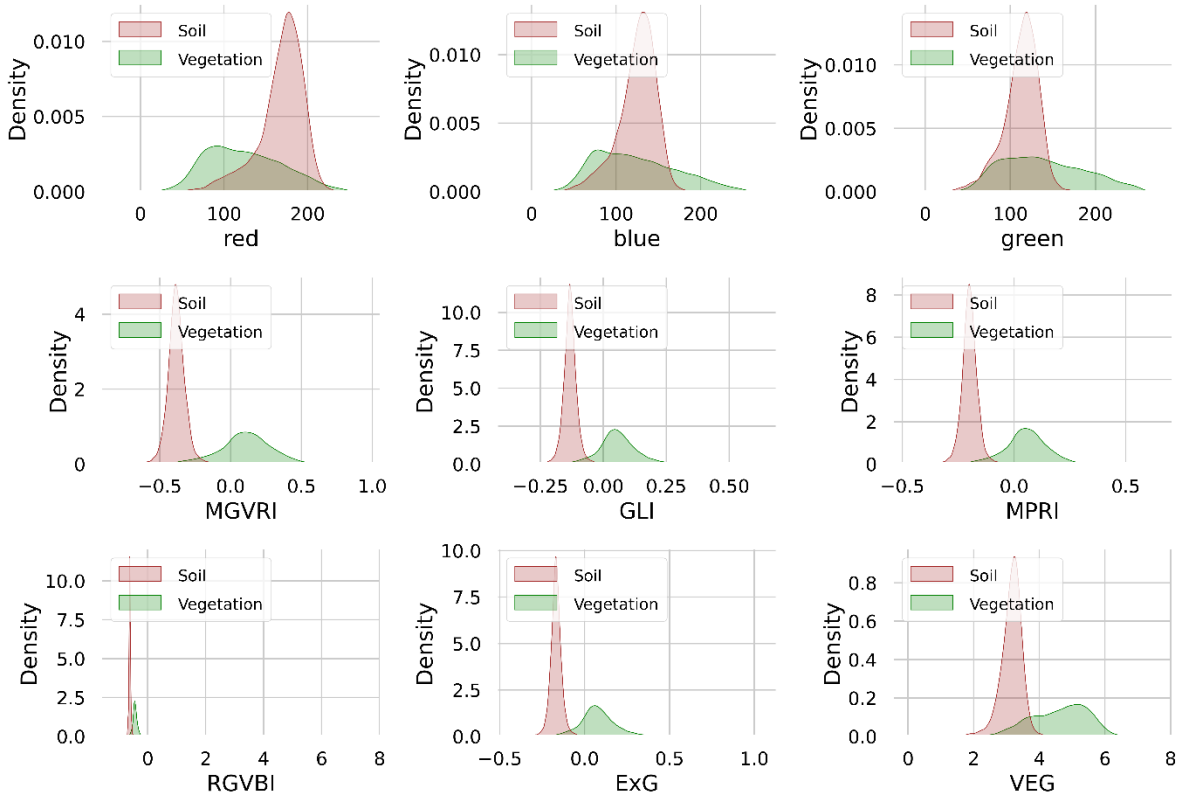

Figure 4. Distribution of pixels related to soil and vegetation by each evaluated indices.

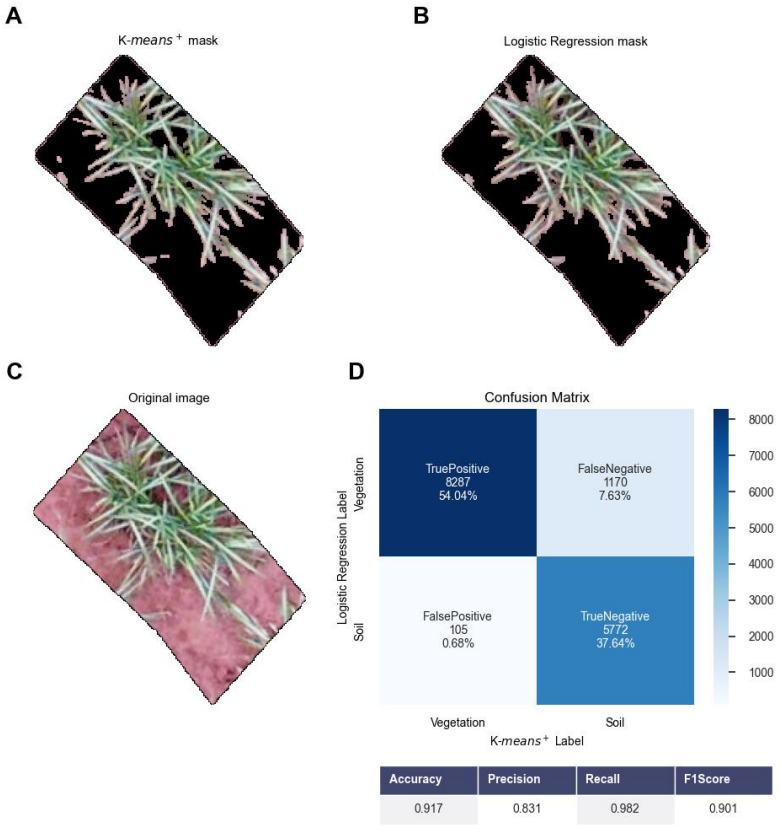

Figure 5. Summary of best-observed performance of the K-means⁺ approach. Comparison between the performance of Logistic Regression and K-means combined with an empirical rule to interpret the clusters (K-means⁺). The table shows the best performance observed for K-means⁺. A) Selection of pixels corresponding to vegetation using K-means⁺. B) Selection of pixels corresponding to vegetation using Logistic Regression. C) Drone Image. D) Confusion Matrix and table with the evaluation metrics of classification.

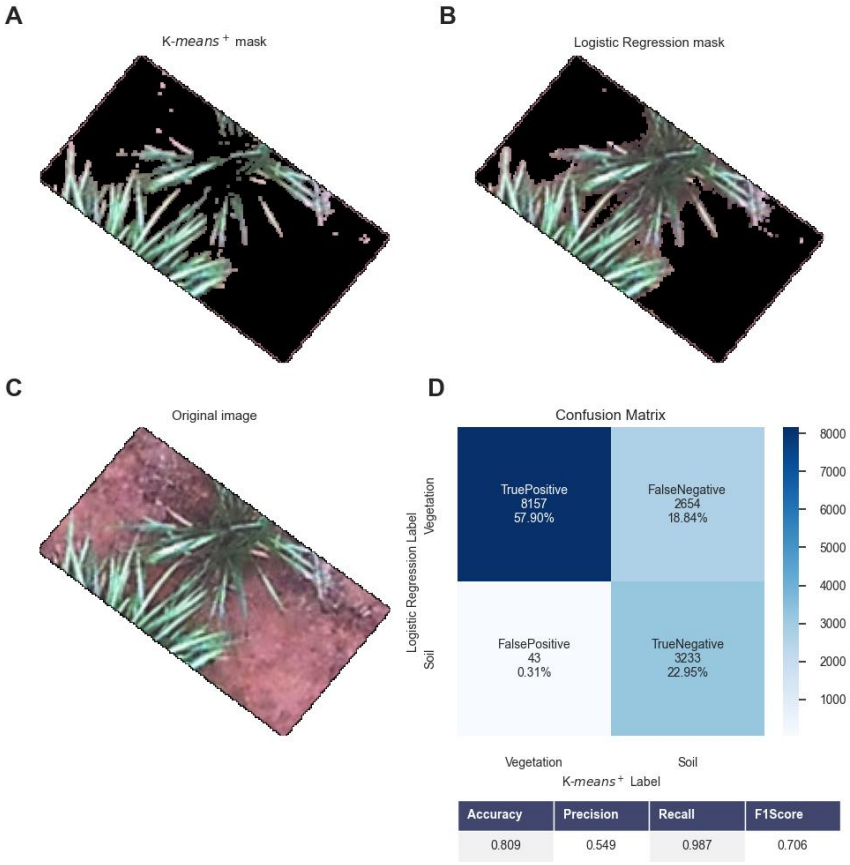

Figure 6. Summary of worse observed performance of the K-means⁺ approach. Comparison between the performance of Logistic Regression and K-means combined with an empirical rule to interpret the clusters (K-means⁺). A) Selection of pixels corresponding to vegetation using K-means⁺. B) Selection of pixels corresponding to vegetation using Logistic Regression. C) Drone Image. D) Confusion Matrix and table with the evaluation metrics of classification.

named labels. Therefore attributes and labels were used to train and validate the pixel-by-pixel classification of the proposed models to perform the image segmentation process.

Supervised models training and evaluation

Three supervised models were considered for the pixels classification process for image segmentation: Random Forest – RF (Breiman, 2001), XGBoost (Chen and Guestrin, 2016), and Logistic Regression – LR (Cox, 1970). The pixels used for model training in image segmentation were evaluated in two scenarios: 1) considering only the R, G, and B bands; 2) using the vegetation indices: GLI, MPRI, RGVBI, ExG, and VEG.

The identification of parameters that maximize the model effectiveness in image segmentation was performed through Gaussian processes using the Bayesian Optimizer (Wu et al., 2019). Based on the previously selected pixels, the algorithm combines them with a priori distribution and, in this way, obtains the posterior distribution, which is then maximized to identify the model's optimal hyperparameters (Wu et al., 2019). In this context, they were optimized using the scikit learn library, the *max depth* and *learning_rate* hyperparameters of the RF classifier, and the *n_estimators*, *min_samples_leaf,* and *max_depth* hyperparameters of the XGBoost classifier. For the LR, all parameters were used in the library standard mode. After obtaining the parameters, the models were evaluated.

Among the supervised models, the one with the best performance was used as the 'standard' image segmentation model. The best model corresponded to the one with the highest accuracy value and the analyses' shortest processing time. The purpose of choosing one of the three supervised models is to use it as a comparison in image segmentation with the K-means algorithm (Sodjinou et al., 2021).

Unsupervised model evaluation

The K-means algorithm minimizes the sum of the distances of each image pixel to the pre-established centroids of the clusters, defining the classes (Sodjinou et al., 2021). As the objective was to segment the image separating vegetation and soil, a k = 2 cluster was defined. In this case, each P pixel in the .tif (Tagged Image File Format) image was related to attributes used in the distance calculation.

Segmentation with K-means was also evaluated in the two scenarios mentioned above (1 - considering only the R, G, and B bands; and 2 - using the vegetation indices: GLI, MPRI, RGVBI, ExG, and VEG) and, later, compared to the segmentation defined with the 'default' model selected in the previous step. In the

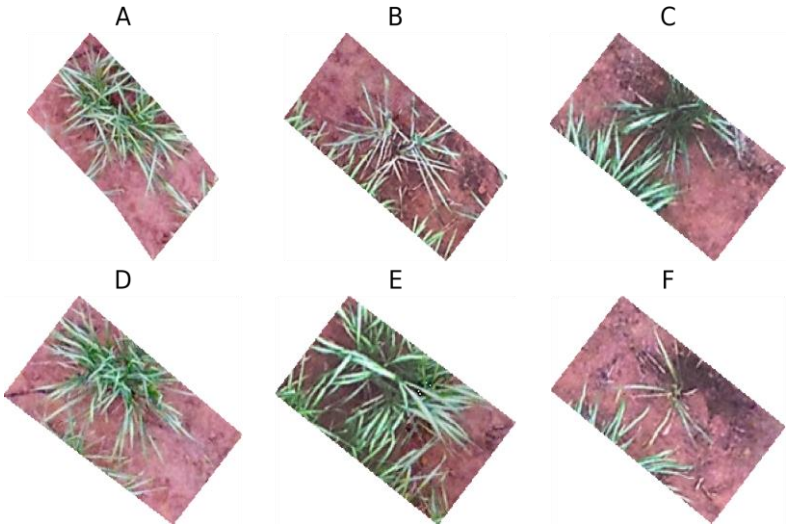

Figure 7. Drone images of experimental sugarcane collected at the Sugarcane Research and Improvement Center (CECA) of the Federal University of Viçosa – UFV.

comparison, we used accuracy, precision, recall, and F1Score (Lu et al., 2021).

To understand such metrics, knowledge of the confusion matrix is essential (Ma et al., 2018). For the binary classification in this research, where the pixel can belong to the soil or vegetation, the confusion matrix allows visualizing the correctly and incorrectly predicted pixels. The confusion matrix has the following elements: correctly predicted (true positive - TP) and incorrectly (false positive - FP) positive values; and negative values correctly predicted (true negative - TN) and incorrectly (false negative - FN). From these elements, the metrics are defined:

$$acuracy = \frac{TP + TN}{TP + FP + TN + FN} \qquad Recall = \frac{TP}{TP + FN}$$

$$Precision = \frac{TP}{TP + TN} \qquad F1Score = \frac{2 \times Precision \times Recall}{Precision + Recall}$$

The accuracy, precision, and recall metrics allow to measure the proportion of pixels correctly predicted in the soil and vegetation classes, the correct percentage among all vegetation pixels correctly predicted in the model, and the percentage of pixels classified as vegetation in the real world. The F1Score metric refers to the harmonic mean of precision and recall. The higher the F1Score value, the better the model performance (Lu et al., 2021).

Empirical rule to interpret the clusters

A new pixel classification approach was defined based on the K-means algorithm. This approach associates the algorithm with an automated criterion to determine the label associated with each group. We call this approach K-means⁺.

When using K-means for grouping pixels in two classes, the labels 0 or 1 are randomly assigned for each class. Thus, label 0 can be assigned to different clusters at each repetition of the analysis. In this work, we defined a criterion to choose which class groups (soil/vegetation) the labels 0 and 1 belong to. The criterion was based on the distribution of the values of the sampled pixels. Based on this evaluation, a decision rule was defined using the average of one of the attributes.

Image segmentation

A black mask was applied to the pixels corresponding to the soil class of all images, leaving the vegetation unmasked in the image after segmentation. This final phase was then called masking. The mask was created using K-means⁺ and the default template. So we compared the performance of the two approaches visually and obtained metrics to evaluate the performance of K-means⁺ considering the classification of the standard model as the true label. The entire process mentioned above in the methodology of this research can be seen in Figure 8.

Resources used for data analysis and processing

To extract the constituent pixels of the data set manually, we used the R software's mapedit library (Appelhans et al., 2020). Subsequently, in the segmentation of the images, with the application and evaluation of the models: RF, XGBoost, K-means, and LR, the Scikit-learn package (Kramer, 2016) of the Python language was used. For the hyperparameter optimization process of the RF and XGBoost models, the Scikit-optimize package also from the Python language was used.

Conclusion

The K-means algorithm presented a similar result to the supervised algorithms in this research. We show that the groups formed using K-means can be interpreted using the averages of the values of the

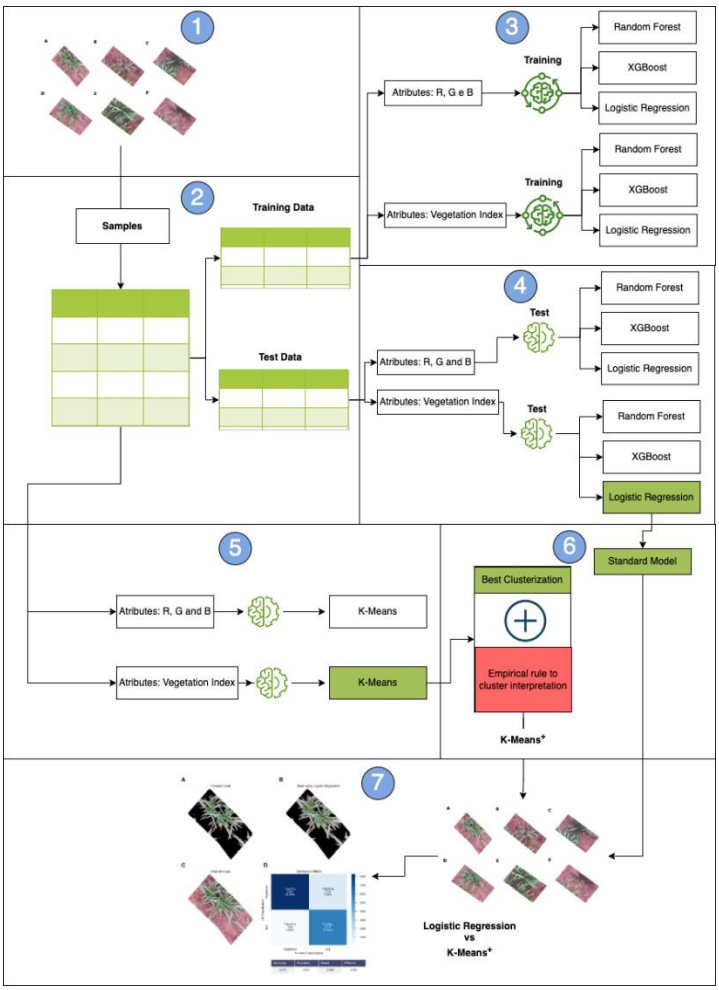

Figure 8. Illustrative diagram of the entire process developed in the research methodology. 1) Drone images. 2) Data processing. 3) Training of supervised models. 4) Evaluation of supervised models. 5) Evaluation of clusterization obtained by K-means algorithm with two sets of attributes. 6) K-means^{+} represent the algorithm K-means combined with an empirical rule to interpret the clusters. 7) Comparison between the best-supervised model and K-means^{+} for an image segmentation task.

MGVRI index within each group of pixels. We presented an approach to an image segmentation process that does not depend on a priori pixel classification. The novel unsupervised approach can classify pixels as efficiently as supervised learning models.

Acknowledgments

The authors are thankful to the Coordenação de Aperfeiçoamento de Pessoal de Nível Superior - Brasil (CAPES) - Finance Code 001, Conselho Nacional de Desenvolvimento Científico e Tecnológico (CNPq), and Fundação de Amparo à Pesquisa de Minas Gerais (FAPEMIG) for the financial support, and the Inter-University Network for the Development of Sugarcane Industry (RIDESA) for providing the images.

Supplementary material

The Python images and scripts used in the research development are available on the GitHub repository: https://github.com/Cristiano2132/article_image_segmentation

References

Adams J, Qiu Y, Xu Y, Schnable J C (2020) Plant segmentation by supervised machine learning methods. Plant Phenome Journal. 3:e20001. https://doi.org/10.1002/PPJ2.20001

Appelhans T, Russell K, Busetto L (2020). _mapedit: Interactive Editing of Spatial Data in R_. R package version 0.6.0, <https://CRAN.R-project.org/package=mapedit>.

Arai K, Barakbah A R (ed) (2007) Hierarchical K-means: an algorithm for centroids initialization for K-means. REP. FAC. SCI. ENGRG. REPORTS OF THE FACULTY OF SCIENCE AND ENGINEERING. 36(1). 25–31.

Bai X, Li X, Fu Z, Lv X, Zhang L (2017) A fuzzy clustering segmentation method based on neighborhood grayscale information for defining cucumber leaf spot disease images. Comput Electron Agr. 136: 157-165. https://doi.org/10.1016/j.compag.2017.03.004

Barbosa B D S, Ferraz G A S, Gonçalves L M, Marin D B, Maciel D T, Ferraz P F P, Rossi G (ed) (2019) RGB vegetation indices applied to grass monitoring: A

qualitative analysis. Agronomy Res. 17(2). https://doi.org/10.15159/AR.19.119

Barth R, IJsselmuiden J, Hemming J, Van Henten E J (2019) Synthetic bootstrapping of convolutional neural networks for semantic plant part segmentation. Comput Electron Agr. 161: 291-304. https://doi.org/10.1016/J.COMPAG.2017.11.040

Bendig J, Yu K, Aasen H, Bolten A, Bennertz S, Broscheit J, Gnyp M L, Bareth G (2015) Combining UAV-based plant height from crop surface models, visible, and near infrared vegetation indices for biomass monitoring in barley. Int J Appl Earth Obs. 39: 79-87. https://doi.org/10.1016/J.JAG.2015.02.012

Breiman L (2001) Random forests. MACH LEARN. 45: 5-32. https://doi.org/10.1023/A:1010933404324

Burgos-Artizzu X P, Ribeiro A, Guijarro M, Pajares G (ed) (2011) Real-time image processing for crop/weed discrimination in maize fields. Comput Electron Agr. 75(2): 337-346. https://doi.org/10.1016/J.COMPAG.2010.12.011

Campbell J, Wynne R (2011) Introduction to remote sensing, 5th edn. GUILFORD PRESS, New York.

Chen T, Guestrin C (2016) XGBoost: A scalable tree boosting system. Associ for Comput Machine. 16: 785: 794. https://doi.org/10.1145/2939672.2939785

Chouhan S S, Singh U P, Sharma U, Jain S (2021) Leaf disease segmentation and classification of Jatropha Curcas L. and Pongamia Pinnata L. biofuel plants using computer vision based approaches. Measurment. 171. https://doi.org/10.1016/j.measurement.2020.108796

Concepcion R, Dadios E, Cuello J, Duarte B (2022) Thermo-gas dynamics affect the leaf canopy shape and moisture content of aquaponic lettuce in a modified partially diffused microclimatic chamber. Sci Hortic. 292: 110649. https://doi.org/10.1016/j.scienta.2021.110649.

Cox D R (1970) ANALYSIS OF BINARY DATA, 2nd edn. Routledge, New York. https://doi.org/10.1201/9781315137391

Ge Y, Bai G, Stoerger V, Schnable J C (2016) Temporal dynamics of maize plant growth, water use, and leaf water content using automated high throughput RGB and hyperspectral imaging. Comput Electron Agr. 127: 625-632. https://doi.org/10.1016/J.COMPAG.2016.07.028

Guerrero J M, Pajares G, Montalvo M, Romeo J, Guijarro M (ed) (2012) Support Vector Machines for crop/weeds identification in maize fields. Expert Syst Appl. 39(12): 11149-11155. https://doi.org/10.1016/J.ESWA.2012.03.040

Guo X, Qiu Y, Nettleton D, Yeh C T, Zheng Z, Hey S, Schnable P S (2021) KAT4IA: K -Means Assisted Training for Image Analysis of Field-Grown Plant Phenotypes. Plant Phenomics. 2021: 1-12. https://doi.org/10.34133/2021/9805489

Hague T, Tillett N D, Wheeler H (ed) (2006) Automated Crop and Weed Monitoring in Widely Spaced Cereals. Precis Agric. 7(1): 21-32. https://doi.org/10.1007/S11119-005-6787-1

Hamuda E, Glavin M, Jones E (2016) A survey of image processing techniques for plant extraction and segmentation in the field. Comput Electron Agr. 125: 184-199. https://doi.org/10.1016/J.COMPAG.2016.04.024

Henke M, Neumann K, Altmann T, Gladilin E (ed) (2021) Semi-automated ground truth segmentation and phenotyping of plant structures using k-means clustering of eigen-colors (Kmseg). Agriculture-SWITZERLAND. 11(11):1098. https://doi.org/10.3390/agriculture11111098

Hunt E R, Cavigelli M, Daughtry C S T, McMurtrey J E, Walthall C L (ed) (2005) Evaluation of Digital Photography from Model Aircraft for Remote Sensing of Crop Biomass and Nitrogen Status. Precis Agric. 6(4): 359-378. https://doi.org/10.1007/S11119-005-2324-5

Kataoka T, Kaneko T, Okamoto H, Hata S (2003) Crop growth estimation system using machine vision. IEEE ASME INT C ADV (AIM 2003). 2: b1079-b1083. https://doi.org/10.1109/AIM.2003.1225492

Kramer O (2016) Scikit-Learn. In: Machine Learning for Evolution Strategies. Studies in Big Data, SPRINGER, Cham. 20. https://doi.org/10.1007/978-3-319-33383-0_5

Lee U, Chang S, Putra G A, Kim H, Kim D H (ed) (2018) An automated, high-throughput plant phenotyping system using machine learning-based plant segmentation and image analysis. Plos ONE. 13(4): e0196615. https://doi.org/10.1371/JOURNAL.PONE.0196615

Louhaichi M, Borman M M, Johnson D E (ed) (2008) Spatially Located Platform and Aerial Photography for Documentation of Grazing Impacts on Wheat. Geocarto Int. 16(1): 65-70. https://doi.org/10.1080/10106040108542184

Lu J, Tan L, Jiang H (ed) (2021) Review on convolutional neural network (CNN) applied to plant leaf disease classification. Agriculture. 11(8):707. https://doi.org/10.3390/agriculture11080707

Lu Y, Young S, Wang H, Wijewardane N (2022) Robust plant segmentation of color images based on image contrast optimization. Comput Electron Agr. 193: 106711. https://doi.org/10.1016/j.compag.2022.106711

Ma J, Du K, Zheng F, Zhang L, Gong Z, Sun Z (2018) A recognition method for cucumber diseases using leaf symptom images based on deep convolutional neural network. Comput Electron Agr. 154: 18-24. https://doi.org/10.1016/j.compag.2018.08.048

Ma J, Du K, Zhang L, Zheng F, Chu J, Sun Z (2017) A segmentation method for greenhouse vegetable foliar disease spots images using color information and region growing. Comput Electron Agr. 142A: 110-117.

https://doi.org/10.1016/j.compag.2017.08.023
Meyer G E, Neto J C (ed) (2008) Verification of color vegetation indices for automated crop imaging applications. Comput Electron Agr. 63(2): 282-293. https://doi.org/10.1016/J.COMPAG.2008.03.009
Reza M N, Na I S, Baek S W, Lee K H (2019) Rice yield estimation based on K-means clustering with graph-cut segmentation using low-altitude UAV images. Biosyst Eng. 177: 109-121. https://doi.org/10.1016/J.BIOSYSTEMSENG.2018.09.014
Sodjinou S G, Mohammadi V, Sanda Mahama A T, Gouton P (ed) (2021) A deep semantic segmentation-based algorithm to segment crops and weeds in agronomic color images. Information Process in Agriculture. 9(3): 355-364. https://doi.org/10.1016/j.inpa.2021.08.003
Taha M F, Abdalla A, Elmasry G, Gouda M, Zhou L, Zhao N, Liang N, Niu Z, Hassanein A, Al-Rejaie S, He Y, Qiu Z (ed) (2022) Using Deep Convolutional Neural Network for Image-Based Diagnosis of Nutrient Deficiencies in Plants Grown in Aquaponics. Chemosensors. 10(2): 45. https://doi.org/10.3390/CHEMOSENSORS10020045
Woebbecke D M, Meyer G E, Von Bargen K, Mortensen D A (ed) (1995) Color Indices for Weed Identification Under Various Soil, Residue, and Lighting Conditions. T ASAE. 38(1): 259-269. https://doi.org/10.13031/2013.27838
Wu J, Chen X Y, Zhang H, Xiong L D, Lei H, Deng S H (ed)(2019) Hyperparameter Optimization for Machine Learning Models Based on Bayesian Optimization. JOURNAL OF ELECTRONIC SCIENCE AND TECHNOLOGY. 17(1): 26-40. https://doi.org/10.11989/JEST.1674-862X.80904120
Yang Z, Willis P, Mueller R (2008) Impact of band-ratio enhanced awifs image to crop classification accuracy. Pecora. 17: 18-20.
Zhang H, Peng Q (2022) PSO and K-means-based semantic segmentation toward agricultural products. Future Gener Comp Sys. 126: 82-87. https://doi.org/10.1016/j.future.2021.06.059
Zhang S, You Z, Wu X (2019) Plant disease leaf image segmentation based on superpixel clustering and EM algorithm. Neural Computing Appl. 31(2): 1225-1232. https://doi.org/10.1007/s00521-017-3067-8
Zheng Y, Kong J, Jin X, Wang X, Su T (ed) (2019) CropDeep: The crop vision dataset for deep-learning-based classification and detection in precision agriculture. Sensors. 19(5):1058. https://doi.org/10.3390/s19051058
Zhou C, Hu J, Xu Z, Yue J, Ye H, Yang G (2020) A Novel Greenhouse-Based System for the Detection and Plumpness Assessment of Strawberry Using an Improved Deep Learning Technique. Front Plant Sci. 11: 559. https://doi.org/10.3389/fpls.2020.00559